

An electrochemical method for the preparation of CaB_6 crystal powder

Xu Wang · Yuchun Zhai

Received: 13 March 2008 / Accepted: 25 March 2009 / Published online: 30 April 2009
© Springer Science+Business Media B.V. 2009

Abstract Calcium boride (CaB_6) crystal powder was prepared by electrolysis in a molten salt electrolyte of 50% CaCl_2 –50% NaCl (molar%) at 750 °C. The current efficiency and product formation rate during the electrolysis were studied based on the experimental data. The electrolytic products including the CaB_6 crystal particles were analyzed by X-ray diffractometry and scanning electron microscopy. Cyclic voltammetry was used to study the electroreduction mechanism of the reactive species. The results demonstrate that the rate of electrolytic reduction is determined by the diffusion rate of the reactive species in the molten salt.

Keywords Calcium boride · Molten salt electrolysis · Current efficiency · Cyclic voltammetry · Electrolytic reduction

1 Introduction

Calcium boride (CaB_6), as a new type of boride ceramic with anti-high energy neutron radiation, has potential application in the nuclear industry. In addition, CaB_6 is a promising deoxidizer in the metallurgical industry due to its excellent deoxidation effect. With the development of CaB_6 applications, the preparation of CaB_6 has attracted much attention. It has been reported that CaB_6 can be prepared by carbothermic and floating zone methods. However, many problems exist in the production process

associated with these methods, such as a high energy consumption and the overall complexity [1–3].

The FFC Cambridge process, on the other hand, is a novel electrochemical method which uses a molten salt electrolyte such as calcium chloride. Compared with conventional metallurgical routes, the FFC Cambridge process is much easier, less expensive and more environmentally friendly. The process involves passing an electric current through a pellet of metal oxide immersed in a molten salt electrolyte.

In this work, we have investigated the direct electrochemical reduction method to produce CaB_6 crystal powder in a CaCl_2 – NaCl molten salt. CaO – B_2O_3 sintered samples were used to prepare the CaB_6 powder without a pelletizing process. This paper reports on the mechanism for the electrolytic reduction of reactants and the cyclic voltammetric analysis of the electrolytic process.

2 Experimental

2.1 Materials and reagents

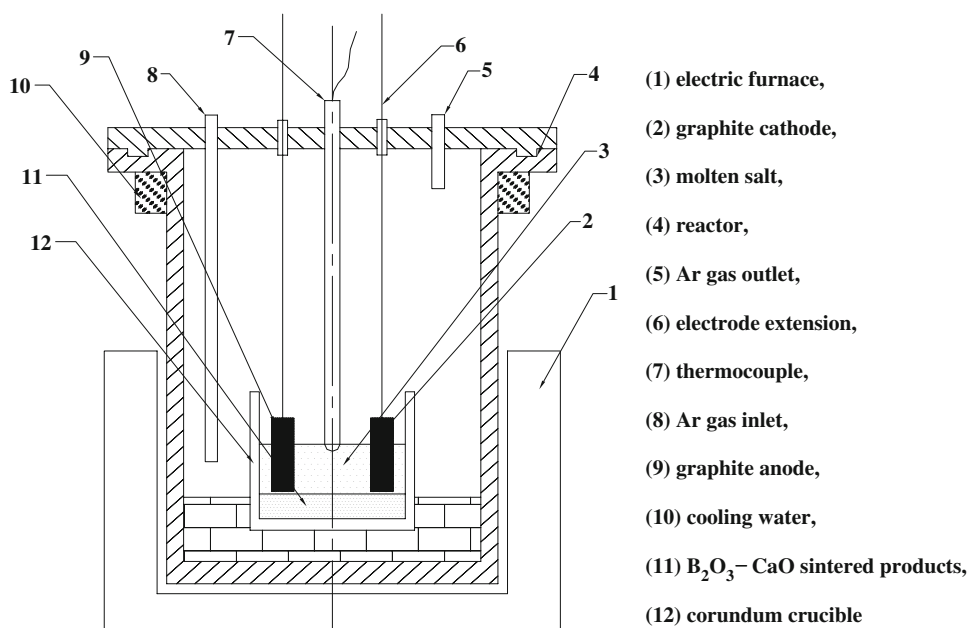
All the chemicals were of analytical grade and used as received without further purification. A mixture prepared from CaCl_2 and NaCl (CaCl_2 : NaCl = 1:1, molar%, 150 g) was dehydrated at 350 °C for 24 h before electrolysis [4, 5]. CaO – B_2O_3 (CaO : B_2O_3 = 1:3, molar%, 10 g) was sintered at 600 °C for 15 h.

2.2 Experimental apparatus

The electrochemical reduction units consisted of Ar gas feeding systems, an electrolysis cell and a temperature controller. Fig. 1 shows the experimental apparatus. The

X. Wang (✉) · Y. Zhai
College of Materials and Metallurgy, Northeastern University,
110004 Shenyang, People's Republic of China
e-mail: wx730313@163.com

Fig. 1 Schematic drawing of the experimental apparatus



electrolysis cell was composed of a resistance furnace, a K-type thermocouple, alumina crucibles, two electrodes, and an Fe–Cr–Al alloy contact conductor. The anode ($\varnothing 10$ mm \times 12 mm) and cathode ($\varnothing 8$ mm \times 12 mm) were made using graphite with high purity and high density.

2.3 Experimental procedure

The pre-electrolysis cell voltage was in the range 1.2–1.5 V, for 2–3 h. The electrolytic cell voltage was 3.0 V, for 20 h. The electrolytic temperature was 750 °C and the electrode spacing was 20 mm. Electrolytic products and CaO– B_2O_3 sintered samples were analyzed by means of X-ray diffraction (XRD, D/max-2500PC, Japan). The morphology and composition of the electrolytic products were analyzed by scanning electron microscopy and energy dispersive spectrometry (SEM and EDS, SSX-550, Japan). An electrochemical workstation (PARSTAT2273, US) was used to analyze the electroreduction mechanism. The electrolysis was carried out under the protection of Ar gas.

3 Results and discussion

Figure 2 presents the XRD patterns of the CaO– B_2O_3 sintered samples. The results show that the CaO– B_2O_3 sintered samples comprise a mixture of B_2O_3 , $Ca_2B_2O_5$, $Ca_3(BO_3)_2$ and CaB_2O_4 . The phase diagram shows that the equilibrium composition should be a mixture of B_2O_3 and $CaO \cdot 2B_2O_3$. Before sintering, CaO and B_2O_3 were in a hydrated state and also absorbed moisture during mixing, resulting in the formation of other borate phases. The CaO–

B_2O_3 sintered samples were reactive species in the process of electrolysis. The standard decomposition potentials of pure $CaCl_2$, NaCl, B_2O_3 and CaO at 750 °C were calculated to be 3.33 V, 3.23 V, 1.73 V, 2.66 V, respectively [6]. The cell voltage for the selective decomposition of the reactive species without decomposition of the $CaCl_2$ –NaCl molten salt was 3.0 V. Pre-electrolysis was carried out in order to remove residual water and some metal impurities from the sintered samples [7].

The melting point of B_2O_3 is 450 °C. In the temperature range 450 to 700 °C, B_2O_3 becomes liquid with greater viscosity and poor liquidity. Under such conditions it is difficult for B_2O_3 to diffuse in the molten salt. It was discovered in the experiment that B_2O_3 has a good liquidity in the temperature range 700 to 800 °C. Normally, the electrolysis temperature should be 100 to 200 °C higher than the molten salt to have better liquidity and good solubility of active substances. The melting point of $CaCl_2$ –NaCl (1:1, molar%) is 501 °C. It was discovered that the $CaCl_2$ –NaCl molten salt has better liquidity in the temperature range 700 to 800 °C. These factors suggest that the experimental temperature should be set at 750 °C.

The CaO– B_2O_3 sintered samples were placed at the bottom of the crucible and covered with the $CaCl_2$ –NaCl molten salt. After completion of the electrolytic run, the electrodes were lifted from the molten salt, cooled in an argon stream, and then removed from the reactor. The electrolytic products were collected from around the cathode, washed with dilute hydrochloric acid and then dried in a cabinet oven. In the process of washing the electrolysis cell, the CaO– B_2O_3 sintered samples were clearly visible at the bottom of the crucible.

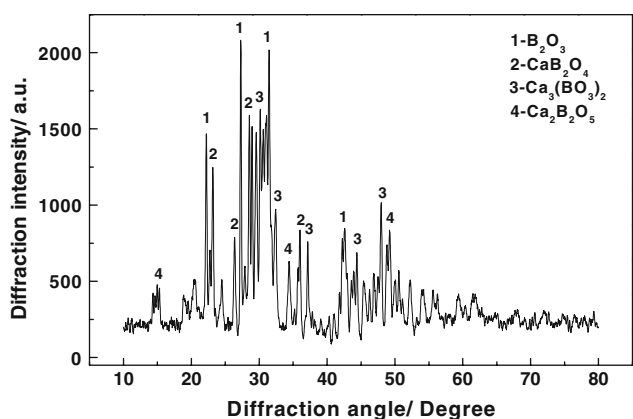


Fig. 2 XRD patterns of the CaO–B₂O₃ (CaO:B₂O₃ = 1:3, molar%) sintered samples

Comparing the changes of the electrode before and after the electrolysis, the cathode exhibited no obvious changes. However, the anode was seriously eroded after completion of the run. We inferred that the anodic product (oxygen gas) combined with the graphite anode and a gaseous mixture (CO₂ and CO) was generated around the anode [8, 9].

Figure 3 presents the XRD patterns of the electrolytic products. The main peaks were assigned to CaB₆, while the minor peaks were characteristic of a number of impurities. An elemental analysis of the electrolytic products revealed that the boron and calcium content in the sintered samples was 97 wt%.

Current–time curves recorded during constant voltage electrolysis are presented in Fig. 4. In the pre-electrolysis, the current increased with time at the beginning of the reaction and reached a maximum at around 0.65 A after only a few minutes. The current then decreased over a period of 100 min to achieve a stable level of 0.42–0.5 A. These changes in the current can be attributed to the removal of residual moisture, metallic and other redox

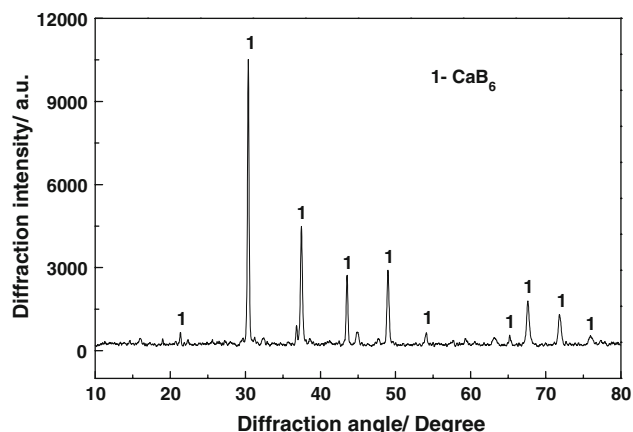


Fig. 3 XRD pattern of the electrolytic products

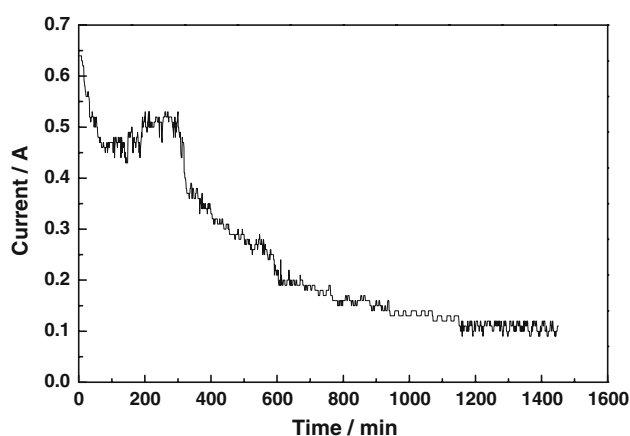


Fig. 4 Time–current curve of the electrolysis reaction

active impurities from the molten salt. In the process of electrolysis, the cell voltage was adjusted to 3.0 V, and the value of the current reached a maximum around 0.55 A and then declined gradually. The gaseous products (O₂, CO and CO₂ gas) discharged from the anode induced tiny current fluctuations. When the electrolysis process was terminated, the background current was around 0.1 A. Further effort is needed to avoid, reduce or eliminate the background current to increase the current efficiency.

The amount of electrolytic products collected during the experiments was 1.06 g (the content of CaB₆ was 97 wt%). The charge passed during the generation of CaB₆ (1.03 g) was $Q_c = 18954.1$ C. According to the time and current data in Fig. 4, the total charge passed during the electrolysis was calculated (using a computer) to be $Q_a = 21760.5$ C. The current efficiency was calculated using the equation:

$$\eta = \frac{Q_c}{Q_a} \times 100\% \tag{1}$$

The current efficiency over the entire electrolysis process was about 87%. Because the amount of CaO–B₂O₃ sintered sample used in the experiment was 10 g, the theoretical output of CaB₆ was calculated to be 3.96 g. According to the actual output of CaB₆ (1.03 g) collected during the experiment, the product formation rate only reached 25%. Based on the experimental fact that the CaO–B₂O₃ sintered samples were deposited at the bottom of the crucible after completion of the electrolytic run, we can further infer that the lower product formation rate is attributed to the slow diffusion of the CaO–B₂O₃ sintered samples in the molten salt [10, 11]. In the high temperature CaCl₂–NaCl molten salt, CaO has better solubility and diffuses more easily in the molten salt through molecular heat-proliferation movement. On the other hand, the higher viscosity and lower solubility of B₂O₃ makes it difficult for this material to diffuse in the molten salt. After sintering,

however, CaO and B₂O₃ reacted together to form boronate and CaO · 2B₂O₃ which lowered the viscosity enabling the CaO · 2B₂O₃ to diffuse slowly in the molten salt.

Figure 5 shows the SEM images of the electrolytic products. Fig. 5a shows typical SEM images of a single crystal grain which is in the shape of a regular cuboid. The results of EDS analysis of this single crystal grain in Fig. 5a are given in Table 1. These indicate that the grain was composed of B and Ca with an atomic ratio of B:Ca = 84:16 (approximate to 6:1). The EDS analyses confirmed that the single crystal grain (Fig. 5a) was CaB₆. From the SEM image shown in Fig. 5b, we consider that the growth mechanism of the crystal grains results in a coherent crystal lattice and a preferred orientation. It can be seen from Fig. 5c that the crystal grains are 1–5 μm in size. Fig. 5d shows an SEM image of the impurities contained in the final product, revealing the irregular and filamentous shapes of the impurities with diameters of around 0.2 μm. Table 2 gives the result of the EDS analysis for the impurities. The main element contained in the impurities is boron with a mass percentage and atomic percentage of 81.27% and 93.38%, respectively. From the EDS analysis, we can further infer that there must be some simple boron substance existing as an intermediate product of the electrolysis. Other observed impurity elements such as Ca, Mg, Al and Si, may originate from the raw material, crucible or reaction environment. Cyclic voltammetry provides a further analysis of the electrolysis process. A cyclic voltammetric curve is shown in Fig. 6. In the analysis, the

Table 1 EDS results of the CaB₆ crystal grain in Fig. 6a

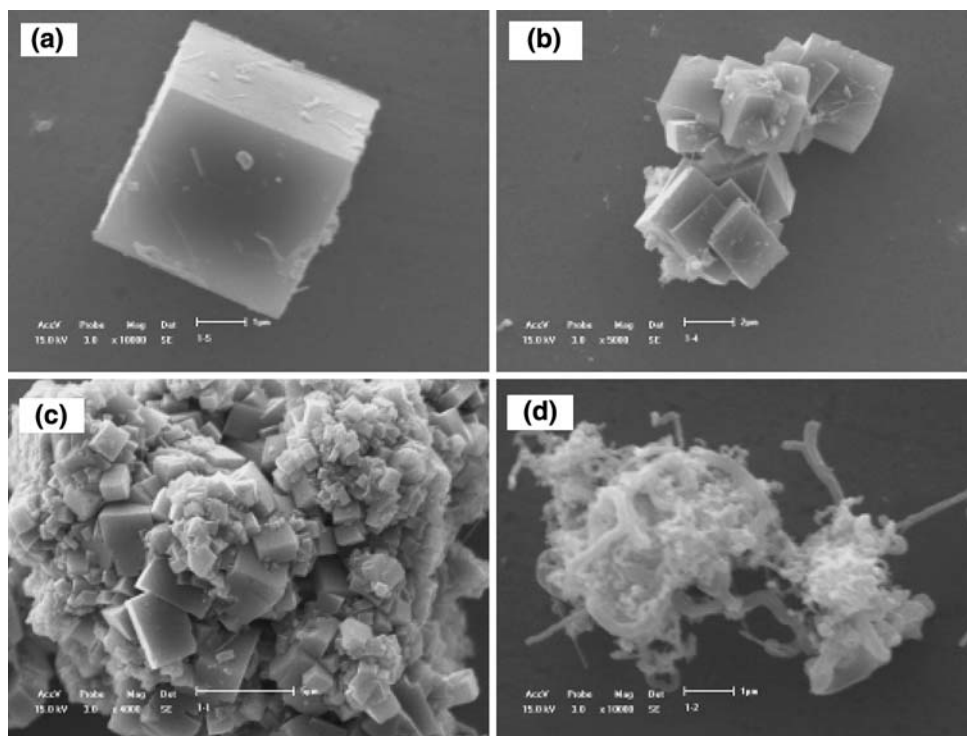
| Element | Intensity | wt% | at. % | K-value | Z | A | F |
|---------|-----------|--------|--------|---------|--------|--------|--------|
| B | 5.678 | 58.407 | 83.888 | 0.2140 | 1.0089 | 1.7057 | 1.0000 |
| Ca | 15.496 | 41.593 | 16.112 | 0.2539 | 1.0559 | 0.9784 | 1.0000 |

Table 2 EDS results of impurities in Fig. 5d

| Element | Intensity | wt% | at. % | K-value | Z | A | F |
|---------|-----------|--------|-------|---------|-------|-------|-------|
| B | 3.152 | 81.271 | 93.38 | 0.1188 | 0.998 | 2.799 | 1.000 |
| Mg | 1.726 | 3.141 | 1.61 | 0.0103 | 1.011 | 1.228 | 0.996 |
| Al | 1.709 | 3.098 | 1.426 | 0.0105 | 1.045 | 1.157 | 0.997 |
| Si | 0.867 | 1.594 | 0.705 | 0.0064 | 1.019 | 1.107 | 0.996 |
| Cl | 0.668 | 2.159 | 0.756 | 0.0083 | 1.087 | 1.008 | 0.993 |
| Ca | 0.512 | 2.136 | 0.662 | 0.0081 | 1.073 | 0.988 | 0.988 |
| Fe | 0.402 | 6.601 | 1.468 | 0.022 | 1.223 | 0.989 | 1.000 |

cathode was used as working electrode and the anode as reference with a 50 mV s⁻¹ scanning rate [12]. The voltammetric scanning was carried out in a range of potentials from -3.2 to 1 V versus CE at a rate of 50 mV s⁻¹. A reduction peak appeared in the negative voltage scanning range of -2.5 to 0 V versus CE. The potential and current of a (end point of the reduction peak), b (the summit point of the reduction peak) and c (the starting point of the reduction peak) are represented by E_a, E_b, E_c, i_a, i_b, i_c, respectively, and these values are given in Table 3.

Fig. 5 SEM micrographs of the electrolytic products



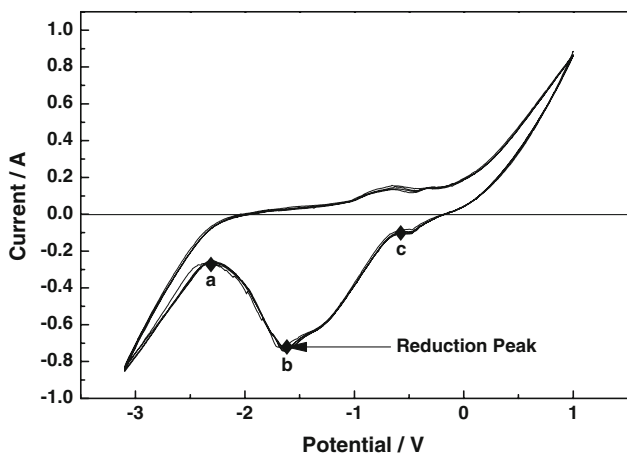


Fig. 6 Cyclic voltammetric curves of the electrolysis reaction

Table 3 Current–Potential value of each point in Fig. 6

| | a | b | c |
|---------------|--------|--------|--------|
| Potential (V) | -2.319 | -1.638 | -0.610 |
| Current (A) | -0.269 | -0.730 | -0.099 |

The analysis and calculations are as follows:

(1) Thermodynamic properties of the system.

Assuming the electrochemical reaction is reversible, the difference between the reduction peak potential (E_p) and the half peak potential ($E_{p/2}$) can be derived using the following equation:

$$|E_p - E_{p/2}| = \frac{2.2RT}{nF} = \frac{2.2 \times 8.31 \times 1023}{20 \times 96485} = 9.69 \times 10^{-3} \text{ V} \quad (2)$$

where R is the gas constant ($8.314 \text{ J mol}^{-1} \text{ K}^{-1}$), T (1023 K) is the temperature in Kelvin, F is the Faraday constant, and n (20) is the transitional number of an electron. Nevertheless, based on the experimental data from Table 3, the true value of $|E_p - E_{p/2}|$ was determined as follows:

$$E_p = -1.028 \text{ V}, E_{p/2} = -0.427 \text{ V}, \text{ and then} \\ |E_p - E_{p/2}| = 0.601 \text{ V} \quad (3)$$

The result indicates that the electrolytic reaction is irreversible.

(2) The transmission coefficient (α) of the active reactants and electrochemical reduction window (E_w).

The transmission coefficient (α) can be obtained from the characteristic equation (4) of the irreversible system:

$$|E_p - E_{p/2}| = \frac{1.857RT}{\alpha F} \quad (4)$$

where $|E_p - E_{p/2}| = 0.601 \text{ V}$, and the value of α was determined to be 2.72.

Electrochemical reduction window (E_w):

$$E_w = |E_b - E_c| = 1.709 \text{ V} \quad (5)$$

(3) The diffusion coefficient (D_0) and concentrations (C_0) of the active reactants:

The diffusion coefficient of the active reactants in the molten salt can be calculated using equation (6):

$$i_p = n \left(2.99 \times 10^5 \alpha^{1/2} A C_0 D_0^{1/2} \nu^{1/2} \right) \quad (6)$$

where i_p is the reduction peak current, A ($1.31 \times 10^{-3} \text{ m}^2$) is the surface area of the working electrode, and ν (50 mV s^{-1}) is the potential scanning rate. $C_0 D_0^{1/2}$ is set as K since C_0 (active ions) is difficult to determine. The value of K in the $\text{CaCl}_2\text{-NaCl}$ molten salt at a temperature of 1023 K is 2.18×10^{-4} . The calculated results indicate that the lower diffusion coefficient (D_0) and the bulk concentration of the reducible ion (C_0) are key factors restricting the rate of electrolysis [13].

After the experiment, a certain amount of salt was removed from the electrolysis cell and dried at $120 \text{ }^\circ\text{C}$ for a period of 24–48 h. Using chemical analysis, the molten salt was found to contain as the main ingredients: $\text{CaCl}_2\text{-NaCl}$, a small amount of B_2O_3 and borate. Since the formation of calcium and boron was not detected directly in the vicinity of the cathode, we deduce that $\text{CaCl}_2\text{-NaCl}$ molten salt mixtures should remain stable at 3.0 V, while CaO , B_2O_3 and borate are decomposed. Moreover, boron and calcium are generated in the vicinity of the cathode, where they then react to form CaB_6 . In addition, the energy spectrum results as shown in Fig. 5d show that the mass percentage and the atomic percentage of B reached 93% and 81%, respectively, which means that there will be a surplus of simple boron after combination with other elements. This surplus boron can be taken as indirect evidence of the formation of boron.

Based on the experimental results, the reaction taking place on the cathode was inferred as follows:

Electrode reactions:



Chemical reaction:



The following reactions on the surface of the anode occurred simultaneously:

Anodic reaction:



Chemical reaction:



illustrate that the electrolytic process is non-reversible and that the lower diffusion.

speed of the reactive species in the molten salt restricts the electrolytic rate.

Acknowledgements The authors extend their thanks to Professor Qian Xu for her interest and useful suggestions.

4 Conclusion

- (1) In the $\text{CaCl}_2\text{--NaCl--CaO--B}_2\text{O}_3$ system, CaB_6 crystal powder was successfully prepared by electrolysis in a molten 50% CaCl_2 –50% NaCl (molar%) electrolyte at 750 °C. The electrolytic cell voltage was 3.0 V. Regular CaB_6 crystals were formed with sizes in the range of 1–5 μm . It was found that the current efficiency can reach 87%, but the product formation rate reached only 25%.
- (2) The electrolytic products including CaB_6 were synthesized from the intermediate products of B and Ca, which were generated from active reactants through complex electrode reactions. The products formed at the anode include O_2 , CO and CO_2 gas. The experimental results and cyclic voltammetry analysis

References

1. Yang LX, Min GH, Yu HS (2003) *Chin Ceram Soc* 7:687
2. Zheng SQ, Min GH, Zou ZD (2001) *Chin Ceram Soc* 2:128
3. Dou ZH, Zhang TA, Hou C (2004) *T Nonferr Metal Soc* 2:322
4. Freidina EB, Fray DJ (2000) *Thermochim Acta* 1:97
5. Freidina EB, Fray DJ (2000) *Thermochim Acta* 1:107
6. Liang YJ, Che YC (1994) *Manual of inorganic thermodynamic data*, 2nd edn. NEUP, Shenyang
7. Zhang MJ, Wang ZW (2006) *Principles and applications of molten electrochemical*, 1st edn. CIP, Beijing
8. Schwandt C, Fray DJ (2005) *Electrochim Acta* 1:66
9. Alexander DTL, Schwandt C, Fray DJ (2006) *Acta Mater* 11:2933
10. Zhang ML, Yan YD, Hou ZY (2007) *J Alloys Compd* 1:362
11. Meng M, Wang DH, Wang WG (2006) *J Alloys Compd* 1:37
12. Li GM, Wang DH, Jin XB (2007) *Electrochem Commun* 8:1951
13. Bard AJ, Faulkner LR (2005) *Electrochemical methods: fundamentals and applications*, 4th edn. CIP, Beijing